Influence of relativistic rotation on the confinement-deconfinement transition within lattice simulation

V. V. Braguta[1,2], A. Yu. Kotov[3], D. D. Kuznedelev[2], A. A. Roenko[1]

[1] Joint Institute for Nuclear Research, Bogoliubov Laboratory of Theoretical Physics
[2] Moscow Institute of Physics and Technology
[3] Jülich Supercomputing Centre

XXXIII International Workshop on High Energy Physics
„Hard Problems of Hadron Physics: Non-Perturbative QCD & Related Quests“
IHEP, Protvino, Russia, 8-12 November 2021

JOINT INSTITUTE FOR NUCLEAR RESEARCH

- In non-central heavy ion collisions creation of QGP with angular momentum is expected.

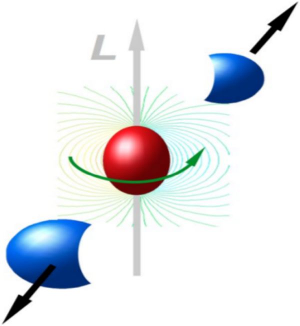

- In non-central heavy ion collisions creation of QGP with angular momentum is expected.
- The rotation occurs with relativistic velocities.

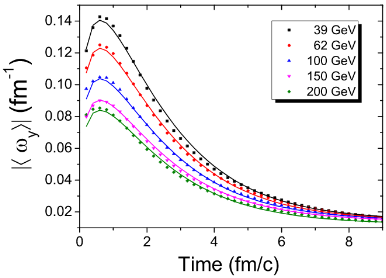

Au+Au, $\quad b = 7$ fm

[Y. Jiang, Z.-W. Lin, and J. Liao, Phys. Rev. C **94**, 044910 (2016), arXiv:1602.06580 [hep-ph]]

$$\omega \sim 0.1 - 0.2\,\mathrm{fm}^{-1} \sim 20 - 40 \ \ \mathrm{MeV}$$

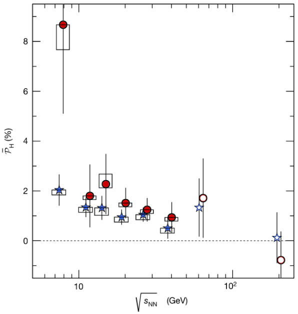

[L. Adamczyk et al. (STAR), Nature **548**, 62–65 (2017), arXiv:1701.06657 [nucl-ex]]

$$\omega \sim 6 \ \mathrm{MeV}$$

- In non-central heavy ion collisions creation of QGP with angular momentum is expected.
- The rotation occurs with relativistic velocities.

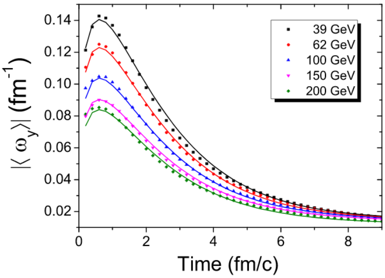

Au+Au, $b = 7$ fm

[Y. Jiang, Z.-W. Lin, and J. Liao, Phys. Rev. C **94**, 044910 (2016), arXiv:1602.06580 [hep-ph]]

$\omega \sim 0.1 - 0.2\,\mathrm{fm}^{-1} \sim 20 - 40$ MeV

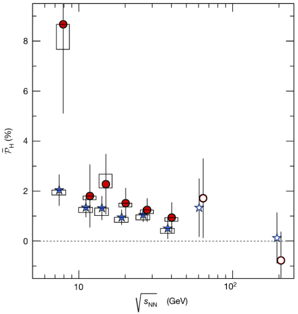

[L. Adamczyk et al. (STAR), Nature **548**, 62–65 (2017), arXiv:1701.06657 [nucl-ex]]

$\omega \sim 6$ MeV

- How does the rotation affect to phase transitions in QCD?

Related papers

Rotation on the lattice (phase transitions were not considered):

- A. Yamamoto and Y. Hirono, Phys. Rev. Lett. **111**, 081601 (2013), arXiv:1303.6292 [hep-lat]

Related papers

Rotation on the lattice (phase transitions were not considered):

- A. Yamamoto and Y. Hirono, Phys. Rev. Lett. **111**, 081601 (2013), arXiv:1303.6292 [hep-lat]

Properties of rotating QCD matter (mostly within NJL, focused on fermions and chiral transition):

- S. Ebihara, K. Fukushima, and K. Mameda, Phys. Lett. B **764**, 94–99 (2017), arXiv:1608.00336 [hep-ph]
- M. Chernodub and S. Gongyo, JHEP **01**, 136 (2017), arXiv:1611.02598 [hep-th]
- X. Wang, M. Wei, Z. Li, and M. Huang, Phys. Rev. D **99**, 016018 (2019), arXiv:1808.01931 [hep-ph]
- H. Zhang, D. Hou, and J. Liao, Chin. Phys. C **44**, 111001 (2020), arXiv:1812.11787 [hep-ph]
- N. Sadooghi, S. M. A. Tabatabaee, and F. Taghinavaz, (2021), arXiv:2108.12760 [hep-ph]
- ...
- Y. Jiang and J. Liao, Phys. Rev. Lett. **117**, 192302 (2016), arXiv:1606.03808 [hep-ph]

Rotation suppress the chiral condensate ($S = 0$), states with $S \neq 0$ are preferable.

Related papers

Rotation on the lattice (phase transitions were not considered):

- A. Yamamoto and Y. Hirono, Phys. Rev. Lett. **111**, 081601 (2013), arXiv:1303.6292 [hep-lat]

Properties of rotating QCD matter (mostly within NJL, focused on fermions and chiral transition):

- S. Ebihara, K. Fukushima, and K. Mameda, Phys. Lett. B **764**, 94–99 (2017), arXiv:1608.00336 [hep-ph]
- M. Chernodub and S. Gongyo, JHEP **01**, 136 (2017), arXiv:1611.02598 [hep-th]
- X. Wang, M. Wei, Z. Li, and M. Huang, Phys. Rev. D **99**, 016018 (2019), arXiv:1808.01931 [hep-ph]
- H. Zhang, D. Hou, and J. Liao, Chin. Phys. C **44**, 111001 (2020), arXiv:1812.11787 [hep-ph]
- N. Sadooghi, S. M. A. Tabatabaee, and F. Taghinavaz, (2021), arXiv:2108.12760 [hep-ph]
- ...
- Y. Jiang and J. Liao, Phys. Rev. Lett. **117**, 192302 (2016), arXiv:1606.03808 [hep-ph]

Rotation suppress the chiral condensate ($S = 0$), states with $S \neq 0$ are preferable.

$\Rightarrow$ Critical temperature decreases due to the rotation.

Related papers

Confinement-deconfinement transition in rotating QCD matter (via phenomenology, effective models):

- Holography: X. Chen et al., JHEP **07**, 132 (2020), arXiv:2010.14478 [hep-ph], A. A. Golubtsova, E. Gourgoulhon, and M. K. Usova, (2021), arXiv:2107.11672 [hep-th]
- Compact QED in 2+1-D M. N. Chernodub, Phys. Rev. D **103**, 054027 (2021), arXiv:2012.04924 [hep-ph]
- HRG model (see Y. Fujimoto's talk): Y. Fujimoto, K. Fukushima, and Y. Hidaka, Phys. Lett. B **816**, 136184 (2021), arXiv:2101.09173 [hep-ph]

Related papers

Confinement-deconfinement transition in rotating QCD matter (via phenomenology, effective models):

- Holography: X. Chen et al., JHEP **07**, 132 (2020), arXiv:2010.14478 [hep-ph], A. A. Golubtsova, E. Gourgoulhon, and M. K. Usova, (2021), arXiv:2107.11672 [hep-th]
- Compact QED in 2+1-D M. N. Chernodub, Phys. Rev. D **103**, 054027 (2021), arXiv:2012.04924 [hep-ph]
- HRG model (see Y. Fujimoto's talk): Y. Fujimoto, K. Fukushima, and Y. Hidaka, Phys. Lett. B **816**, 136184 (2021), arXiv:2101.09173 [hep-ph]

$\Rightarrow$ Critical temperature also decreases due to the rotation.

Related papers

Confinement-deconfinement transition in rotating QCD matter (via phenomenology, effective models):

- Holography: X. Chen et al., JHEP **07**, 132 (2020), arXiv:2010.14478 [hep-ph], A. A. Golubtsova, E. Gourgoulhon, and M. K. Usova, (2021), arXiv:2107.11672 [hep-th]
- Compact QED in 2+1-D M. N. Chernodub, Phys. Rev. D **103**, 054027 (2021), arXiv:2012.04924 [hep-ph]
- HRG model (see Y. Fujimoto's talk): Y. Fujimoto, K. Fukushima, and Y. Hidaka, Phys. Lett. B **816**, 136184 (2021), arXiv:2101.09173 [hep-ph]

$\Rightarrow$ Critical temperature also decreases due to the rotation.

Taking into account the contribution of rotating gluons to NJL model:

- Y. Jiang, (2021), arXiv:2108.09622 [hep-ph]

The running effective coupling $G(\omega)$ is introduced.

Confinement-deconfinement transition in rotating QCD matter (via phenomenology, effective models):

- Holography: X. Chen et al., JHEP **07**, 132 (2020), arXiv:2010.14478 [hep-ph], A. A. Golubtsova, E. Gourgoulhon, and M. K. Usova, (2021), arXiv:2107.11672 [hep-th]
- Compact QED in 2+1-D M. N. Chernodub, Phys. Rev. D **103**, 054027 (2021), arXiv:2012.04924 [hep-ph]
- HRG model (see Y. Fujimoto's talk): Y. Fujimoto, K. Fukushima, and Y. Hidaka, Phys. Lett. B **816**, 136184 (2021), arXiv:2101.09173 [hep-ph]

$\Rightarrow$ Critical temperature also decreases due to the rotation.

Taking into account the contribution of rotating gluons to NJL model:

- Y. Jiang, (2021), arXiv:2108.09622 [hep-ph]

The running effective coupling $G(\omega)$ is introduced.
$\Rightarrow$ Critical temperature increases due to the rotation.

- QCD (at thermal equilibrium) is investigated in the reference frame which rotates with the system with angular velocity Ω .
- In this reference frame there appears an external gravitational field

$$g_{\mu\nu} = \begin{pmatrix} 1 - r^2\Omega^2 & \Omega y & -\Omega x & 0 \\ \Omega y & -1 & 0 & 0 \\ -\Omega x & 0 & -1 & 0 \\ 0 & 0 & 0 & -1 \end{pmatrix} .$$

- The partition function is[1]

$$Z = \int D\psi\, D\bar{\psi}\, DA \exp\big(- S_G[A,\Omega] - S_F[\bar{\psi},\psi,A,\Omega]\big) . \qquad (1)$$

The rotation affect both gluon and quark degrees of freedom!

[1] A. Yamamoto and Y. Hirono, Phys. Rev. Lett. **111**, 081601 (2013), arXiv:1303.6292 [hep-lat].

- QCD (at thermal equilibrium) is investigated in the reference frame which rotates with the system with angular velocity Ω .
- In this reference frame there appears an external gravitational field

$$g_{\mu\nu} = \begin{pmatrix} 1 - r^2\Omega^2 & \Omega y & -\Omega x & 0 \\ \Omega y & -1 & 0 & 0 \\ -\Omega x & 0 & -1 & 0 \\ 0 & 0 & 0 & -1 \end{pmatrix}.$$

- The partition function is[1]

$$Z = \int D\psi\, D\bar{\psi}\, DA\, \exp\left(- S_G[A,\Omega] - S_F[\bar{\psi},\psi,A,\Omega]\right). \qquad (1)$$

The rotation affect both gluon and quark degrees of freedom!

Interplay between these effects may lead to non-trivial results.

[1] A. Yamamoto and Y. Hirono, Phys. Rev. Lett. **111**, 081601 (2013), arXiv:1303.6292 [hep-lat].

- Tolman-Ehrenfest effect: In gravitational field the temperature isn't a constant in space at thermal equilibrium:

$$T(r)\sqrt{g_{00}} = const\,,$$

Rotating reference frame: temperature

- Tolman-Ehrenfest effect: In gravitational field the temperature isn't a constant in space at thermal equilibrium:

$$T(r)\sqrt{g_{00}} = const\,,$$

- For the rotation one has

$$T(r)\sqrt{1 - r^2\Omega^2} = const \equiv T\,,$$

- One could expect, that the rotation effectively warm up the periphery of the modeling volume

$$T(r) > T(r = 0),$$

and as a result, from kinematics, the critical temperature should decreases.

The Euclidean gluon action can be written as

$$S_G = \frac{1}{4g^2} \int d^4x \, \sqrt{g_E} \, g_E^{\mu\nu} g_E^{\alpha\beta} F^a_{\mu\alpha} F^a_{\nu\beta} \, . \tag{2}$$

Substituting the $(g_E)_{\mu\nu}$ to formula (2) one gets

$$\begin{aligned} S_G = \frac{1}{2g^2} \int d^4x \, \Big[&(1 - r^2\Omega^2) F^a_{xy} F^a_{xy} + (1 - y^2\Omega^2) F^a_{xz} F^a_{xz} + (1 - x^2\Omega^2) F^a_{yz} F^a_{yz} + \\ &+ F^a_{x\tau} F^a_{x\tau} + F^a_{y\tau} F^a_{y\tau} + F^a_{z\tau} F^a_{z\tau} - \\ &- 2iy\Omega (F^a_{xy} F^a_{y\tau} + F^a_{xz} F^a_{z\tau}) + 2ix\Omega (F^a_{yx} F^a_{x\tau} + F^a_{yz} F^a_{z\tau}) - 2xy\Omega^2 F^a_{xz} F^a_{zy} \Big] \, . \end{aligned}$$

The Euclidean gluon action can be written as

$$S_G = \frac{1}{4g^2} \int d^4x \, \sqrt{g_E} \, g_E^{\mu\nu} \, g_E^{\alpha\beta} \, F^a_{\mu\alpha} F^a_{\nu\beta} \, . \tag{2}$$

Substituting the $(g_E)_{\mu\nu}$ to formula (2) one gets

$$S_G = \frac{1}{2g^2} \int d^4x \, \Big[(1 - r^2\Omega^2) F^a_{xy} F^a_{xy} + (1 - y^2\Omega^2) F^a_{xz} F^a_{xz} + (1 - x^2\Omega^2) F^a_{yz} F^a_{yz} + \\ + F^a_{x\tau} F^a_{x\tau} + F^a_{y\tau} F^a_{y\tau} + F^a_{z\tau} F^a_{z\tau} - \\ - 2iy\Omega (F^a_{xy} F^a_{y\tau} + F^a_{xz} F^a_{z\tau}) + 2ix\Omega (F^a_{yx} F^a_{x\tau} + F^a_{yz} F^a_{z\tau}) - 2xy\Omega^2 F^a_{xz} F^a_{zy} \Big] .$$

Sign problem

- The Euclidean action is complex-valued function!
- The Monte–Carlo simulations are conducted with imaginary angular velocity $\Omega_I = -i\Omega$.
- The results are analytically continued to the region of the real angular velocity.

The lattice gluon action can be written as

$$S_G = \beta \sum_x \Big((1 + r^2\Omega_I^2)(1 - \frac{1}{N_c}\text{Re Tr } \bar{U}_{xy}) + (1 + y^2\Omega_I^2)(1 - \frac{1}{N_c}\text{Re Tr } \bar{U}_{xz}) +$$
$$+ (1 + x^2\Omega_I^2)(1 - \frac{1}{N_c}\text{Re Tr } \bar{U}_{yz}) + 3 - \frac{1}{N_c}\text{Re Tr } (\bar{U}_{x\tau} + \bar{U}_{y\tau} + \bar{U}_{z\tau}) -$$
$$- \frac{1}{N_c}\text{Re Tr } \big(y\Omega_I(\bar{V}_{xy\tau} + \bar{V}_{xz\tau}) - x\Omega_I(\bar{V}_{yx\tau} + \bar{V}_{yz\tau}) + xy\Omega_I^2 \bar{V}_{xzy} \big) \Big),$$

where $\beta = 2N_c/g^2$,

$\bar{U}_{\mu\nu}$ denotes clover-type average of four plaquettes,

$\bar{V}_{\mu\nu\rho}$ is asymmetric chair-type average of 8 chair.

$\overline{U}_{\mu\nu} = \frac{1}{4}$ 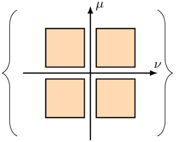

$\overline{V}_{\mu\nu\rho} = \frac{1}{8}$ 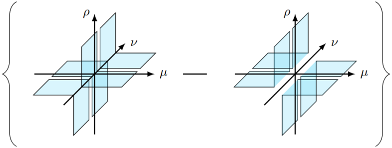

Rotating gluodynamics: lattice setup

- Simulation is performed on the lattice $N_t \times N_z \times N_s^2 \;\; (N_s = N_x = N_y)$, which rotates around z-axis.
- The system should be limited in the directions, which are orthogonal to the rotation axis: $\Omega_I (N_s - 1) a/\sqrt{2} < 1$

Rotating gluodynamics: lattice setup

- Simulation is performed on the lattice $N_t \times N_z \times N_s^2$ $(N_s = N_x = N_y)$, which rotates around z-axis.
- The system should be limited in the directions, which are orthogonal to the rotation axis: $\Omega_I (N_s - 1) a/\sqrt{2} < 1$

$$\Downarrow$$

- The boundary conditions in directions x, y have to be treated carefully! The results depend on BC for any approach. (PBC are used in directions t, z.)

- Simulation is performed on the lattice $N_t \times N_z \times N_s^2 \;\; (N_s = N_x = N_y)$, which rotates around z-axis.
- The system should be limited in the directions, which are orthogonal to the rotation axis: $\Omega_I (N_s - 1) a/\sqrt{2} < 1$

$$\Downarrow$$

- The boundary conditions in directions x, y have to be treated carefully! The results depend on BC for any approach. (PBC are used in directions t, z.)

The following types of BC were systematically checked:

- Open b.c. – OBC
  - All $U_{\mu\nu}$, $V_{\mu\nu\rho}$, which contain links sticking out of the lattice, excluded.
  - Does not break any symmetries.
  - $U_P = 1$ for all $P \in$ out; or $F_{\mu\nu} = 0 \quad \Rightarrow \quad$ „low“ temperature on the boundary.

Rotating gluodynamics: lattice setup

- Simulation is performed on the lattice $N_t \times N_z \times N_s^2$ $(N_s = N_x = N_y)$, which rotates around z-axis.
- The system should be limited in the directions, which are orthogonal to the rotation axis: $\Omega_I(N_s - 1)a/\sqrt{2} < 1$

$$\Downarrow$$

- The boundary conditions in directions x, y have to be treated carefully! The results depend on BC for any approach. (PBC are used in directions t, z.)

The following types of BC were systematically checked:

- Open b.c. – OBC
  - All $U_{\mu\nu}$, $V_{\mu\nu\rho}$, which contain links sticking out of the lattice, excluded.
  - Does not break any symmetries.
  - $U_P = 1$ for all $P \in$ out; or $F_{\mu\nu} = 0$ $\Rightarrow$ „low“ temperature on the boundary.
- Periodic b.c. – PBC
  - The velocity distribution is not periodic.

Rotating gluodynamics: lattice setup

- Simulation is performed on the lattice $N_t \times N_z \times N_s^2$ $(N_s = N_x = N_y)$, which rotates around z-axis.
- The system should be limited in the directions, which are orthogonal to the rotation axis: $\Omega_I (N_s - 1) a/\sqrt{2} < 1$

$$\Downarrow$$

- The boundary conditions in directions x, y have to be treated carefully! The results depend on BC for any approach. (PBC are used in directions t, z.)

The following types of BC were systematically checked:

- Open b.c. – OBC
  - All $U_{\mu\nu}$, $V_{\mu\nu\rho}$, which contain links sticking out of the lattice, excluded.
  - Does not break any symmetries.
  - $U_P = 1$ for all $P \in$ out; or $F_{\mu\nu} = 0$ $\Rightarrow$ „low“ temperature on the boundary.
- Periodic b.c. – PBC
  - The velocity distribution is not periodic.
- Dirichlet b.c. – DBC
  - $U_\mu(x) = \hat{1}$ for all $x, x + \mu \in$ boundary
  - Violate $\mathbb{Z}_3$ center symmetry.
  - $L(x, y) = 3$ on the boundary $\Rightarrow$ „high“ temperature on the boundary.

Rotating gluodynamics: critical temperature

The Polyakov loop is an order parameter. The lattice version is defined as usual:

$$L(\vec{x}) = \mathrm{Tr}\left[\prod_{\tau=0}^{N_t-1} U_4(\vec{x},\tau)\right], \qquad L = \frac{1}{N_s^2 N_z}\sum_{\vec{x}} L(\vec{x})\,. \tag{3}$$

In confinement $\langle L\rangle = 0$; in deconfinement $\langle L\rangle \neq 0$ ($\mathbb{Z}_3$ center symmetry is broken).

The critical temperature T_c is determined using the Polyakov loop susceptibility

$$\chi = N_s^2 N_z\left(\langle |L|^2\rangle - \langle |L|\rangle^2\right), \tag{4}$$

by means of the Gaussian fit.

Rotating gluodynamics: critical temperature

The Polyakov loop is an order parameter. The lattice version is defined as usual:

$$L(\vec{x}) = \mathrm{Tr}\left[\prod_{\tau=0}^{N_t-1} U_4(\vec{x},\tau)\right], \qquad L = \frac{1}{N_s^2 N_z}\sum_{\vec{x}} L(\vec{x}) . \tag{3}$$

In confinement $\langle L \rangle = 0$; in deconfinement $\langle L \rangle \neq 0$ ($\mathbb{Z}_3$ center symmetry is broken).

The critical temperature T_c is determined using the Polyakov loop susceptibility

$$\chi = N_s^2 N_z \left(\langle |L|^2 \rangle - \langle |L| \rangle^2\right) , \tag{4}$$

by means of the Gaussian fit.

- Non-periodic b.c. changes the critical temperature $T_c(0)$
  - $T_c(0)^{OBC} > T_c(0)^{PBC}$
  - $T_c(0)^{DBC} < T_c(0)^{PBC}$
- With $N_s/N_t \to \infty$ their influence wanes, and $T_c(0) \to T_c(0)^{(PBC)}$
- The spatial distributions of the local Polyakov loop $L(x,y) = \frac{1}{N_z}\sum_z L(x,y,z)$ show that the boundary is screened.

Rotating gluodynamics: Polyakov loop distribution (OBC)

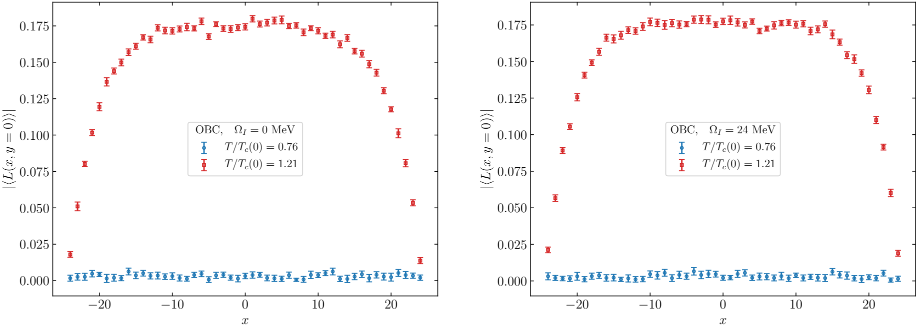

Figure: The local Polyakov loop $|\langle L(x, y)\rangle|$ as a function of coordinate for OBC and $\Omega_I = 0$ MeV (left), $\Omega_I = 24$ MeV (right). Points with $x \neq 0, y = 0$ from the lattice $8 \times 24 \times 49^2$ are shown.

- The local Polyakov loop $|\langle L(x, y)\rangle|$ is zero for all spatial points in the confinement phase, both with and without rotation $\Rightarrow$ Polyakov loop still acts as the order parameter.
- In deconfinement phase the boundary is screened.

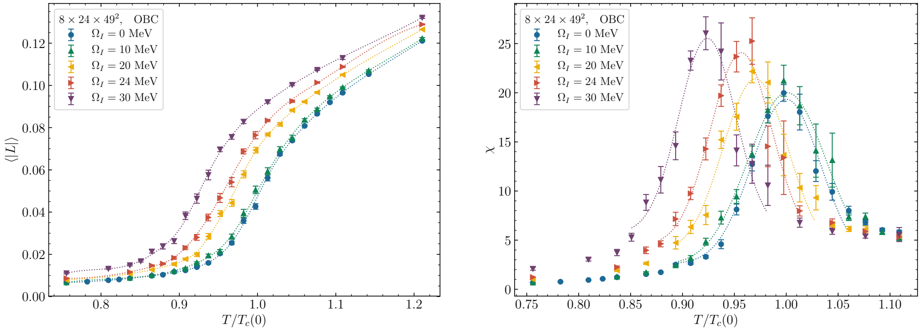

(a) (b)

Figure: The Polyakov loop (a) and Polyakov loop susceptibility (b) as a function of temperature for different values of imaginary angular velocity Ω_I. The results are obtained on the lattice $8 \times 24 \times 49^2$.

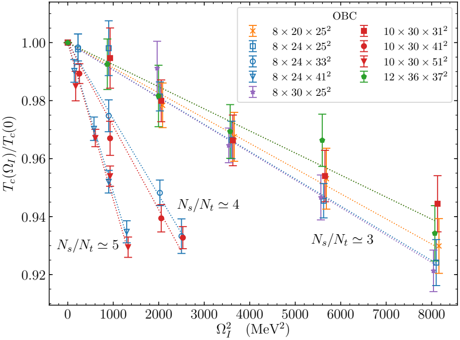

T_c depends on Ω_I^2 and is well described by

$$\frac{T_c(\Omega_I)}{T_c(0)} = 1 - C_2\Omega_I^2$$

- The coefficient C_2 depends on the transverse lattice size (N_s/N_t) and is almost independent of both the lattice spacing and the lattice size along the rotation axis (N_z/N_t).

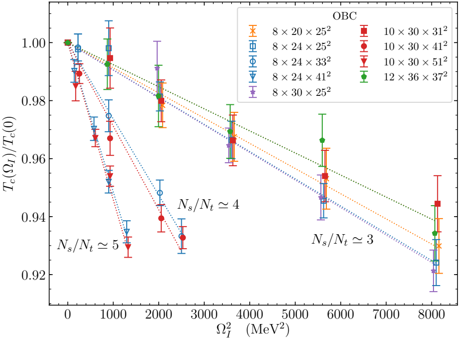

T_c depends on Ω_I^2 and is well described by

$$\frac{T_c(\Omega_I)}{T_c(0)} = 1 - C_2\Omega_I^2$$

$$\Downarrow \quad (\Omega_I^2 = -\Omega^2)$$

$$\frac{T_c(\Omega)}{T_c(0)} = 1 + C_2\Omega^2$$

The critical temperature increases with the angular velocity ($C_2 > 0$)

- The coefficient C_2 depends on the transverse lattice size (N_s/N_t) and is almost independent of both the lattice spacing and the lattice size along the rotation axis (N_z/N_t).

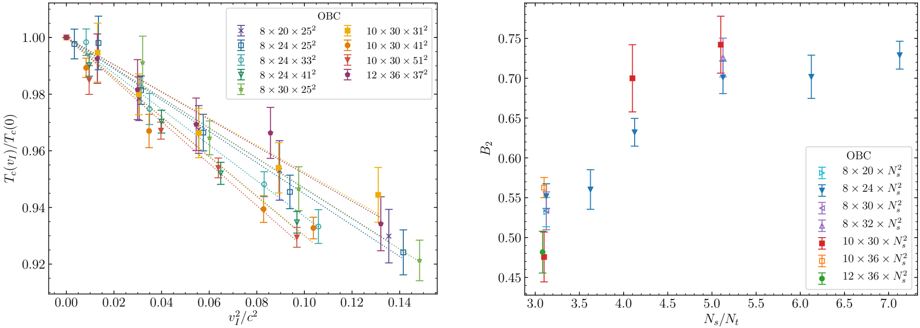

The linear velocity on the boundary $v_I = \Omega_I\,(N_s-1)\,a(\beta_c)/2$

$$\frac{T_c(v_I)}{T_c(0)} = 1 - B_2\frac{v_I^2}{c^2}$$

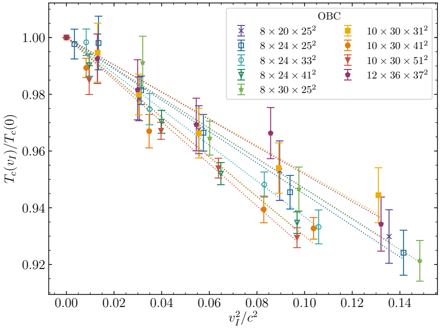

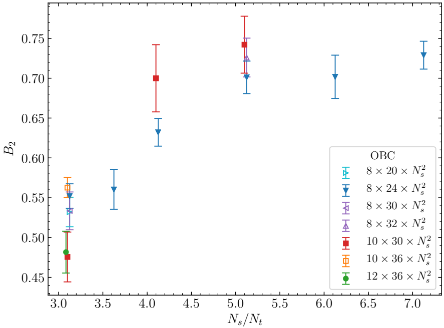

The linear velocity on the boundary $v_I = \Omega_I\,(N_s - 1)\,a(\beta_c)/2$

$$\frac{T_c(v_I)}{T_c(0)} = 1 - B_2\frac{v_I^2}{c^2} \qquad \Longrightarrow \qquad \frac{T_c(v)}{T_c(0)} = 1 + B_2\frac{v^2}{c^2}$$

- The critical temperature increases with the angular velocity.
- For lattices with sufficiently large N_s and OBC the coefficient is $B_2 \sim 0.7$.

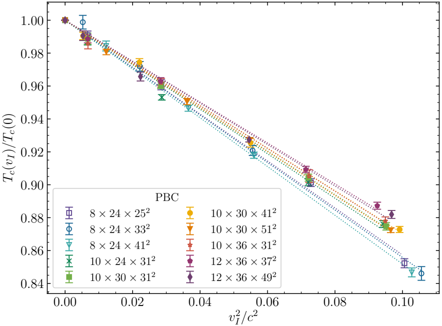

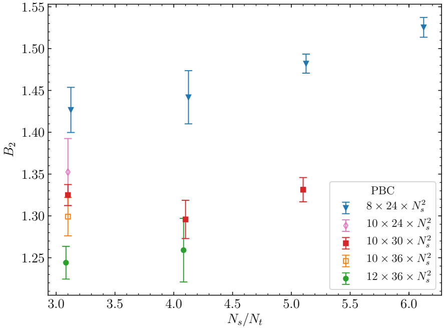

The linear velocity on the boundary $v_I = \Omega_I\,(N_s - 1)\,a(\beta_c)/2$

$$\frac{T_c(v_I)}{T_c(0)} = 1 - B_2 \frac{v_I^2}{c^2} \qquad \Longrightarrow \qquad \frac{T_c(v)}{T_c(0)} = 1 + B_2 \frac{v^2}{c^2}$$

- The critical temperature increases with the angular velocity.
- The results for the finest lattices with $N_t = 10, 12$ are close to each others, and for PBC the coefficient is $B_2 \sim 1.3$.

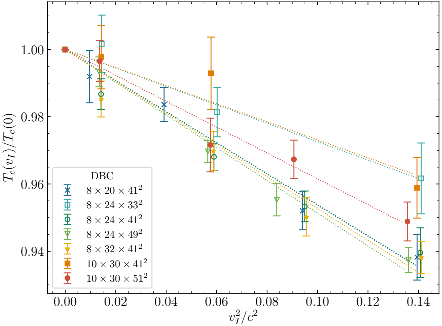

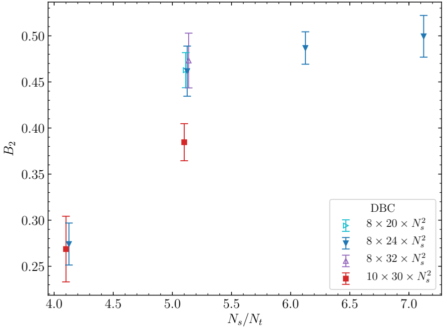

The linear velocity on the boundary $v_I = \Omega_I \, (N_s - 1) \, a(\beta_c)/2$

$$\frac{T_c(v_I)}{T_c(0)} = 1 - B_2 \frac{v_I^2}{c^2} \qquad \Longrightarrow \qquad \frac{T_c(v)}{T_c(0)} = 1 + B_2 \frac{v^2}{c^2}$$

- The critical temperature increases with the angular velocity.
- For lattices with sufficiently large N_s and DBC the coefficient goes to plateau $B_2 \sim 0.5$.

Rotating gluodynamics: susceptibility scaling

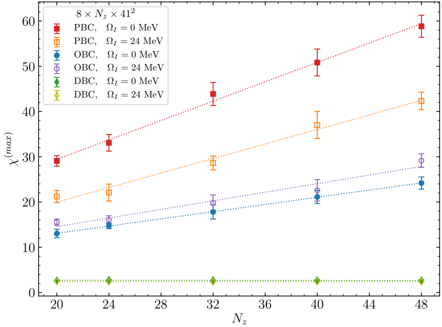

Figure: The height of the susceptibility peak for various lattices $8 \times N_z \times 41^2$ and zero/nonzero angular velocities.

Rotation does not change the order of the phase transition (in studied region of Ω):

- OBC: $\chi^{(max)} \sim V$
- PBC: $\chi^{(max)} \sim V$
- DBC: $\chi^{(max)} \sim const$

The rotation affect both gluon and quark degrees of freedom.

$$Z = \int D\psi \, D\bar{\psi} \, DA \, \exp\big(- S_G[A, \Omega] - S_F[\bar{\psi}, \psi, A, \Omega] \big) \, . \tag{5}$$

Rotating QCD: quark lattice action

The rotation affect both gluon and quark degrees of freedom.

$$Z = \int D\psi\, D\bar{\psi}\, DA \,\exp\big(- S_G[A,\Omega] - S_F[\bar{\psi},\psi,A,\Omega]\big)\,. \qquad (5)$$

There is the sign problem for the initial lattice quark action. After the same substitution ($\Omega = -i\Omega_I$) it has the following form

$$\begin{aligned} S_F = \sum_{x_1,x_2} \bar{\psi}(x_1) \Bigg\{ \delta_{x_1,x_2} - \kappa \Big[&(1-\gamma^x) T_{x+} + (1+\gamma^x) T_{x-} \\ &+ (1-\gamma^y) T_{y+} + (1+\gamma^y) T_{y-} + (1-\gamma^z) T_{z+} + (1+\gamma^z) T_{z-} \\ &+ (1-\gamma^\tau) \exp\left(ia\Omega_I \frac{\sigma^{12}}{2} \right) T_{\tau+} + (1+\gamma^\tau) \exp\left(- ia\Omega_I \frac{\sigma^{12}}{2} \right) T_{\tau-} \Big] \Bigg\} \psi(x_2)\,, \end{aligned} \qquad (6)$$

where $\kappa = 1/(8+2am)$, $T_{\mu+} = U_\mu(x_1)\delta_{x_1+\mu,x_2}$, $T_{\mu-} = U_\mu(x_1)\delta_{x_1-\mu,x_2}$ and

$$\gamma^x = \gamma^1 - y\Omega_I\gamma^4, \quad \gamma^y = \gamma^2 + x\Omega_I\gamma^4, \quad \gamma^z = \gamma^3, \quad \gamma^\tau = \gamma^4.$$

The Monte-Carlo simulations with dynamical fermions ($N_f = 2$ Wilson fermions) for an imaginary angular velocity were performed.

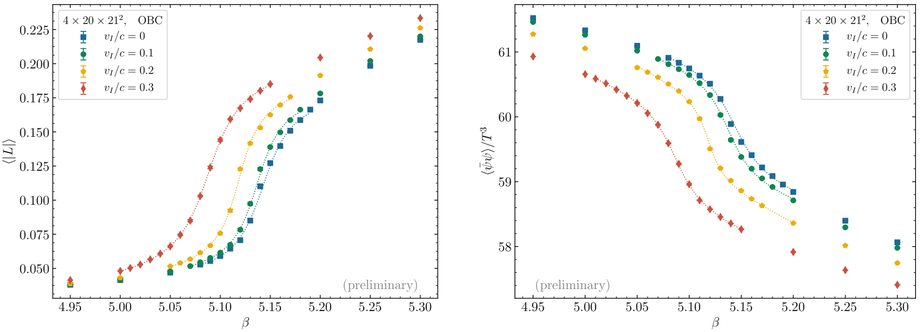

(a) (b)

Figure: The Polyakov loop (a) and the chiral condensate (b) as a function of β for different values of imaginary angular velocity Ω_I. Lattice $4 \times 20 \times 21^2$, the hopping parameter $\kappa = 0.170$ ($m_\pi \simeq 690$ MeV, $T \simeq 171$ MeV for $\beta = 5.15$).

- Critical couplings β_c for both chiral transition and confinement-deconfinement transition decrease.

Rotating QCD: Open boundary conditions (preliminary results)

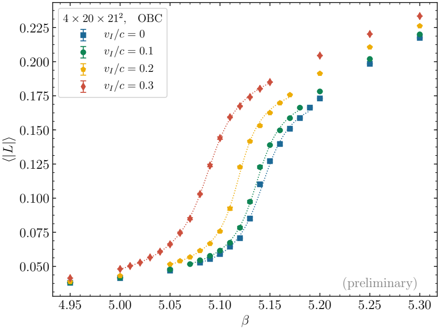

(a)

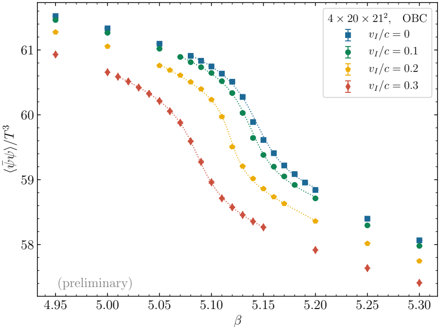

(b)

Figure: The Polyakov loop (a) and the chiral condensate (b) as a function of β for different values of imaginary angular velocity Ω_I. Lattice $4\times20\times21^2$, the hopping parameter $\kappa=0.170$ ($m_\pi\simeq690$ MeV, $T\simeq171$ MeV for $\beta=5.15$).

- Critical couplings β_c for both chiral transition and confinement-deconfinement transition decrease.

One can split the full action as $S_G(\Omega_G)+S_F(\Omega_F)$ and rotate each part separately!

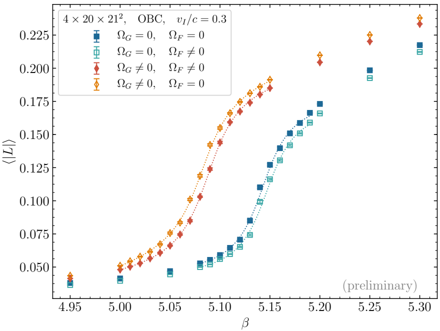

(a)

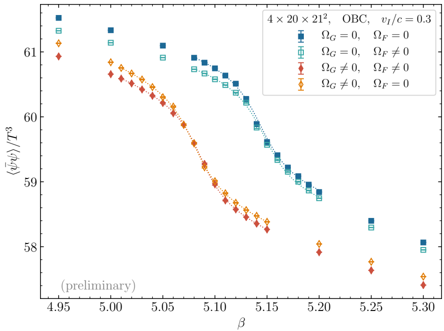

(b)

Figure: The Polyakov loop (a) and the chiral condensate (b) as a function of β for different values of imaginary angular velocity Ω_I. Lattice $4 \times 20 \times 21^2$, the hopping parameter $\kappa = 0.170$.

- Rotation of fermions and gluons separately has the opposite influence on the critical coupling (temperature).

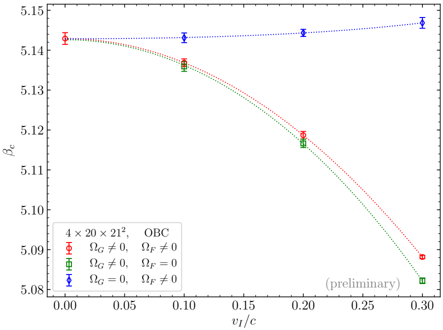

(a)

Figure: The critical value β_c as function of imaginary linear velocity on the boundary.

- Rotation of fermions and gluons separately has the opposite influence on the critical coupling (temperature).

Rotating QCD (preliminary results)

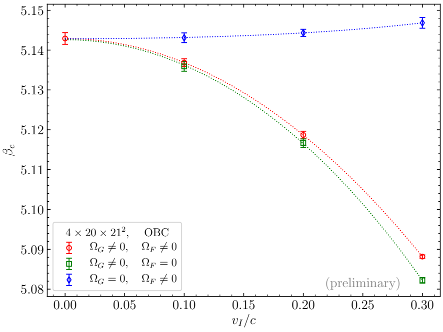

(a)

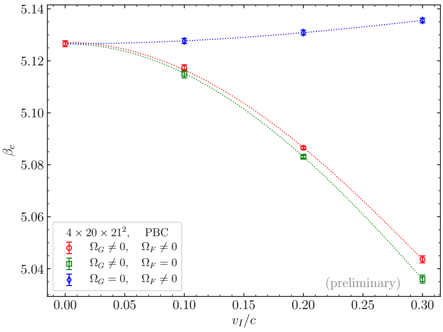

(b)

Figure: The critical value β_c as function of imaginary linear velocity on the boundary.

- Rotation of fermions and gluons separately has the opposite influence on the critical coupling (temperature).
- The results are qualitatively the same for OBC and PBC.

Conclusions

- The critical temperature of the confinement/deconfinement transition in gluodynamics increases with angular velocity ($v \propto \Omega$)

$$\frac{T_c(v)}{T_c(0)} = 1 + B_2 \frac{v^2}{c^2}\,.$$

It's not Tolman-Ehrenfest effect! (NB: Gluons have spin-1)

- The result does not depend on the boundary conditions used: for OBC $B_2 \sim 0.7$, for PBC $B_2 \sim 1.3$ and for DBC $B_2 \sim 0.5$
- It should be noted, that NJL (and other phenomenological models) predicts that critical temperature decreases due to the rotation. But taking into account the contribution of rotating gluons leads to an increase in T_c.
- Preliminary results for QCD show that the separate rotation of quarks and gluons has the opposite influence on β_c. (for $m_\pi \sim 690$ MeV gluons win: $T_c \nearrow$).

See the details in:

- V. V. Braguta, A. Y. Kotov, D. D. Kuznedelev, and A. A. Roenko, Oct. 2021, arXiv:2110.12302 [hep-lat]
- V. V. Braguta, A. Y. Kotov, D. D. Kuznedelev, and A. A. Roenko, Phys. Rev. D **103**, 094515 (2021), arXiv:2102.05084 [hep-lat]
- V. V. Braguta, A. Y. Kotov, D. D. Kuznedelev, and A. A. Roenko, JETP Lett. **112**, 6–12 (2020)

Thank you for your attention!

NJL with $G(\omega)$

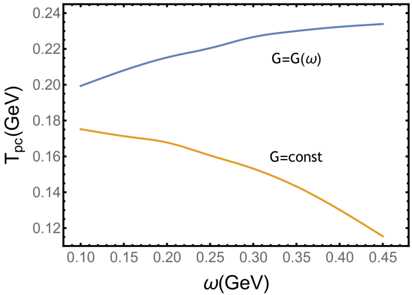

Figure: form Y. Jiang, (2021), arXiv:2108.09622 [hep-ph]

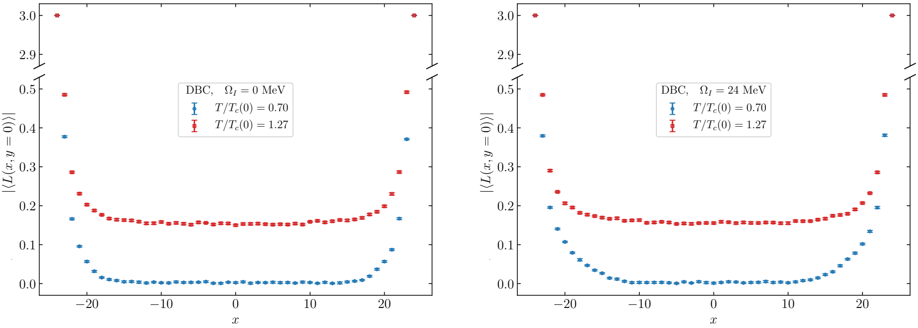

Figure: The local Polyakov loop $|\langle L(x,y)\rangle|$ as a function of coordinate for OBC and $\Omega_I = 0$ MeV (left), $\Omega_I = 24$ MeV (right). Points with $x \neq 0, y = 0$ from the lattice $8 \times 24 \times 49^2$ are shown.

- The local Polyakov loop $|\langle L(x,y)\rangle|$ is equal three on the boundary in both phases.
- The boundary is screened.

Rotating gluodynamics: Polyakov loop distribution (PBC)

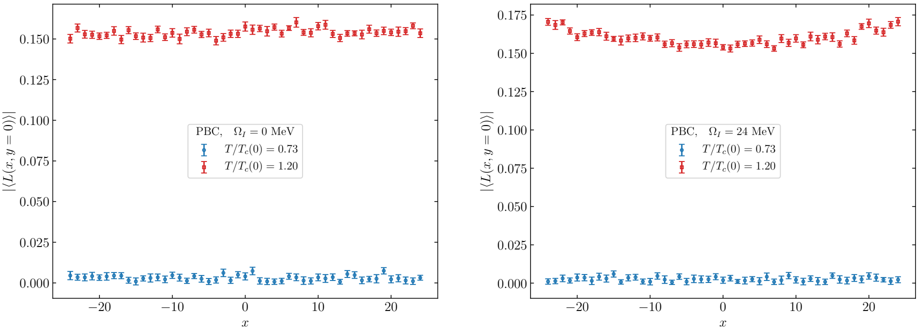

Figure: The local Polyakov loop $|\langle L(x, y)\rangle|$ as a function of coordinate for OBC and $\Omega_I = 0$ MeV (left), $\Omega_I = 24$ MeV (right). Points with $x \neq 0, y = 0$ from the lattice $8 \times 24 \times 49^2$ are shown.

- The local Polyakov loop $|\langle L(x, y)\rangle|$ is zero for all spatial points in the confinement phase, both without rotation and with nonzero angular velocity.
- The local Polyakov loop demonstrates weak dependence on the coordinate in the deconfinement phase.

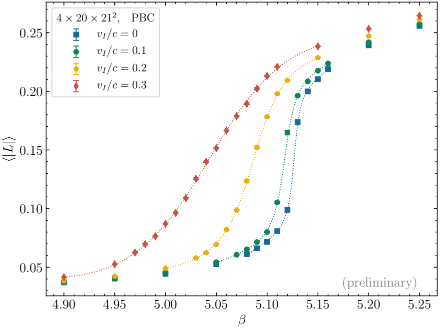

(a)

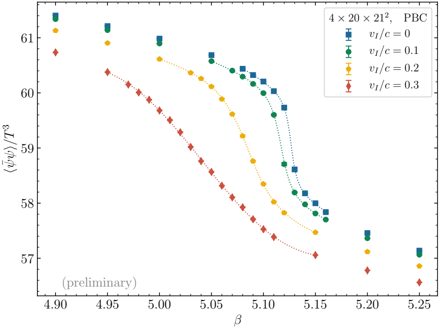

(b)

Figure: The Polyakov loop (a) and the chiral condensate (b) as a function of β for different values of imaginary angular velocity Ω_I. Lattice $4 \times 20 \times 21^2$, the hopping parameter $\kappa = 0.170$ ($m_\pi \simeq 690$ MeV, $T \simeq 171$ MeV for $\beta = 5.15$).

- Critical couplings β_c for both chiral transition and confinement-deconfinement transition decrease.

Rotating QCD: Periodic boundary conditions (preliminary results)

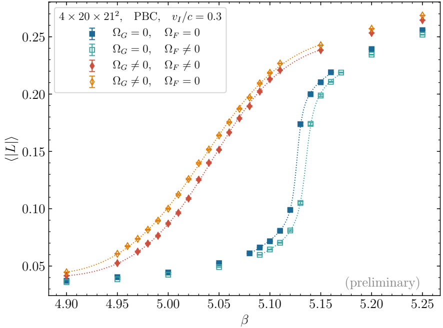

(a)

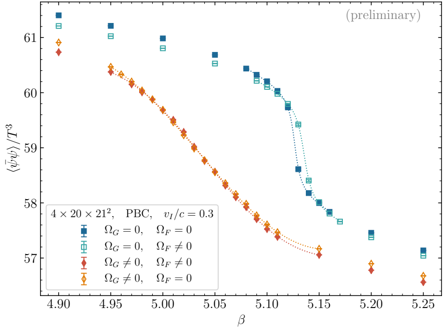

(b)

Figure: The Polyakov loop (a) and the chiral condensate (b) as a function of β for different values of imaginary angular velocity Ω_I. Lattice $4 \times 20 \times 21^2$, the hopping parameter $\kappa = 0.170$.

- Rotation of fermions and gluons separately has the opposite influence on the critical coupling (temperature).

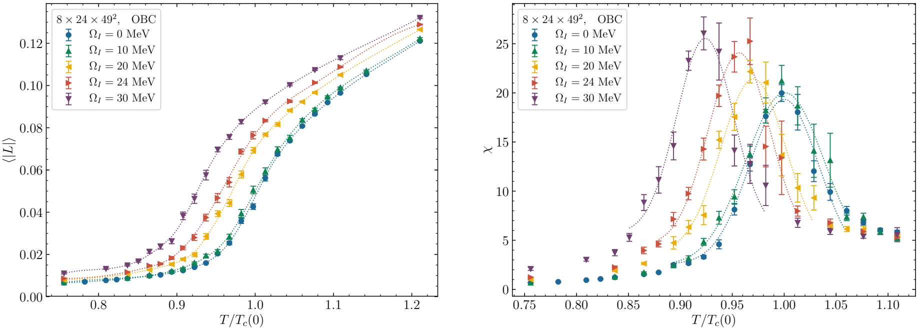

(a) (b)

Figure: The Polyakov loop (a) and Polyakov loop susceptibility (b) as a function of temperature for different values of imaginary angular velocity Ω_I. The results are obtained on the lattice $8 \times 24 \times 49^2$.

- The height of the peak $\chi^{(max)}$ slightly grows with angular velocity for OBC.

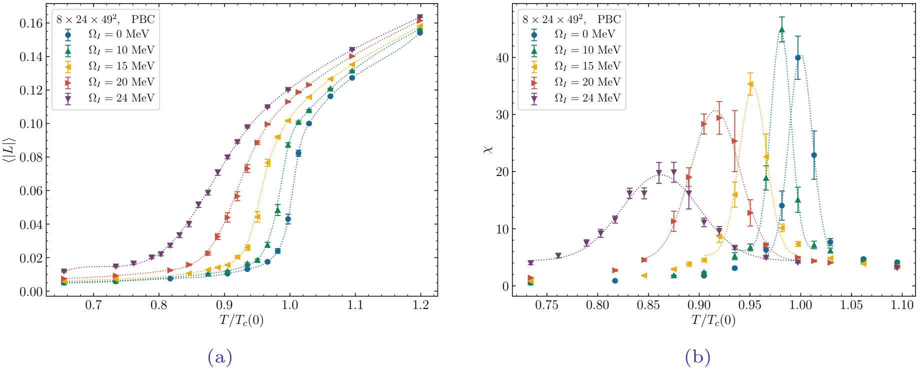

Figure: The Polyakov loop (a) and Polyakov loop susceptibility (b) as a function of temperature for different values of imaginary angular velocity Ω_I. The results are obtained on the lattice $8 \times 24 \times 49^2$.

- The height of the peak $\chi^{(max)}$ falls down with angular velocity.

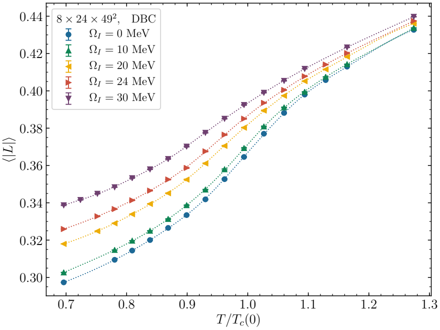

(a)

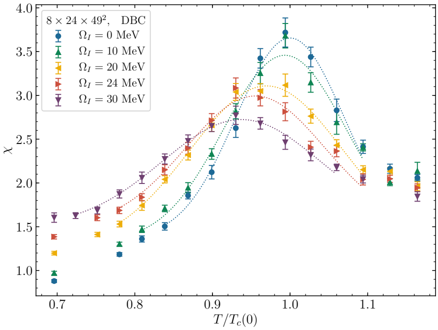

(b)

Figure: The Polyakov loop (a) and Polyakov loop susceptibility (b) as a function of temperature for different values of imaginary angular velocity Ω_I. The results are obtained on the lattice $8 \times 24 \times 49^2$.

- The height of the Polyakov loop susceptibility $\chi^{(max)}$ falls down with rotation.
- Polyakov loop is not zero for low temperatures. Contribution from boundary is $\delta L_{b.c.} = 12(N_s - 1)/N_s^2$, or $\delta L_{b.c.} \simeq 0.24$.